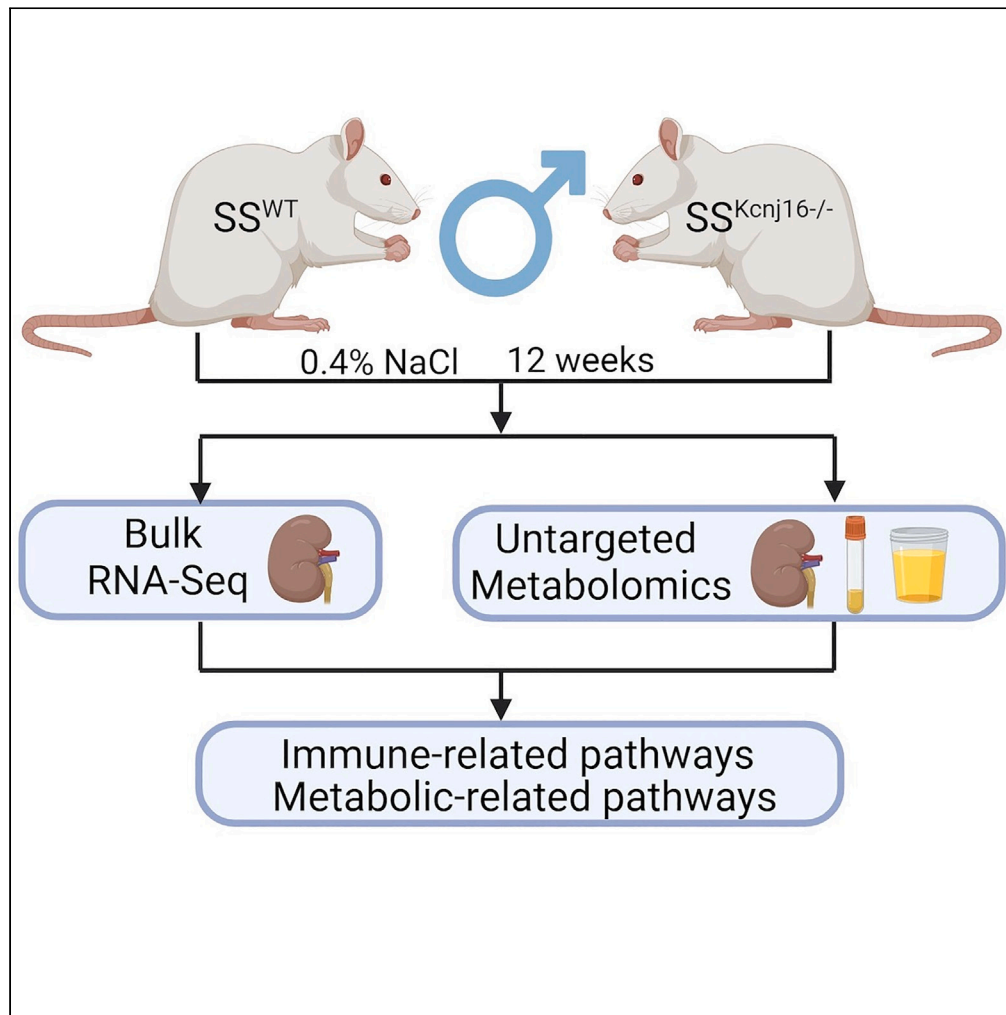# iScience

Article

Deletion of *Kcnj16* altered transcriptomic and metabolomic profiles of Dahl salt-sensitive rats

Biyang Xu,
Lashodya V.
Dissanayake,
Vladislav
Levchenko, Adrian
Zietara, Olha
Kravtsova,
Alexander
Staruschenko

bxu@usf.edu (B.X.)
staruschenko@usf.edu (A.S.)

Highlights

SS$^{Kcnj16-/-}$ rats showed
altered transcriptomic and
metabolomic profiles

Multi-omics suggested
suppressed immune and
altered metabolic
pathways

iScience

Article

Deletion of *Kcnj16* altered transcriptomic and metabolomic profiles of Dahl salt-sensitive rats

Biyang Xu,[1],* Lashodya V. Dissanayake,[1] Vladislav Levchenko,[1] Adrian Zietara,[1] Olha Kravtsova,[1] and Alexander Staruschenko[1,2,3,4],*

SUMMARY

The inwardly rectifying K⁺ channel $K_{ir}5.1$ (*Kcnj16*) is essential in renal salt handling and blood pressure control. However, the underlying mechanisms are not fully understood. Here, we integrated transcriptomics and metabolomics to comprehensively profile the changes in genes and metabolites in the Dahl salt-sensitive (SS) rat lacking *Kcnj16* to identify potential mechanisms. Consistent with the phenotype of knockout (KO) rats, the transcriptomic profile predicted reduced blood pressure, kidney damage, and increased ion transport. Canonical pathway analysis suggested activation of metabolic-related pathways while suppression of immune response-related pathways in KO rats. Untargeted metabolomic analysis revealed different metabolic profiles between wild-type (WT) and KO rats. Integration of transcriptomic and metabolomic profiles suggested altered tricarboxylic acid (TCA) cycle, amino acid metabolism, and reactive oxygen species (ROS) metabolism that are related to SS hypertension. In conclusion, besides increased ion transport, our data suggest suppressed immune response-related and altered metabolic-related pathways of SS rats lacking $K_{ir}5.1$.

INTRODUCTION

In the kidney, discretionary Na⁺ reabsorption and K⁺ secretion in the distal nephron and collecting duct are responsible for fine-tuning of water and electrolyte homeostasis.[1,2] Inwardly rectifying K⁺ (K_{ir}) channels, specifically homomeric $K_{ir}4.1$ and heteromeric $K_{ir}4.1/K_{ir}5.1$ channels, play a dominant role in determining the basolateral K⁺ conductance and the membrane potential.[2–5] In humans, loss-of-function variants in *KCNJ10* ($K_{ir}4.1$) are associated with EAST/SeSAME syndrome, which is characterized by renal salt wasting with hypokalemic alkalosis associated with epilepsy, ataxia, and sensorineural deafness.[6,7] More recent studies also suggested that defects in *KCNJ16* ($K_{ir}5.1$) cause hypokalemia, salt wasting, disturbed acid-base homeostasis, and sensorineural deafness in patients.[5,8]

Our previous results using *Kcnj16* knockout (KO) rats based on the Dahl salt-sensitive (SS) rat model demonstrated that compared to wild-type (WT) SS rats, KO rats displayed severe hypokalemia, reduced blood pressure, and kidney damage, suggesting the essential role of $K_{ir}5.1$ in renal salt handling and blood pressure control.[3] Dahl SS rats were chosen since this strain represents an excellent model for studying salt-induced hypertension and kidney injury.[9–12] The KO rats also had an altered renin-angiotensin-aldosterone system,[13] acute and chronic pH homeostasis,[14] and respiratory function.[15] Furthermore, KO rats experienced audiogenic seizures, which were prevented by dietary potassium supplementation.[16] Despite the essential role of $K_{ir}5.1$ in renal salt handling and blood pressure control, the underlying mechanisms are still not fully understood.

With the recent technological and methodological developments, the omics approach (genomics, epigenomics, transcriptomics, proteomics, and metabolomics) has drawn more and more attention as it offers a more complete picture of all heritable factors influencing certain diseases.[17] For a complex disease like hypertension, numerous studies have used the omics approach to identify new underlying mechanisms, suggesting the correlation between altered transcriptomic and metabolomic profiling with hypertension.[18–22]

To the best of our knowledge, no study has used an omics approach to investigate how $K_{ir}5.1$ affects blood pressure and kidney damage. Thus, here, we aim to integrate transcriptomic and metabolomic approaches to identify further potential mechanisms contributing to the effect of $K_{ir}5.1$ on renal salt handling and blood pressure control in SS hypertension.

[1]Department of Molecular Pharmacology & Physiology, Morsani College of Medicine, University of South Florida, Tampa, FL, USA
[2]Hypertension and Kidney Research Center, University of South Florida, Tampa, FL, USA
[3]James A. Haley Veteran's Hospital, Tampa, FL, USA
[4]Lead contact
*Correspondence: bxu@usf.edu (B.X.), staruschenko@usf.edu (A.S.)
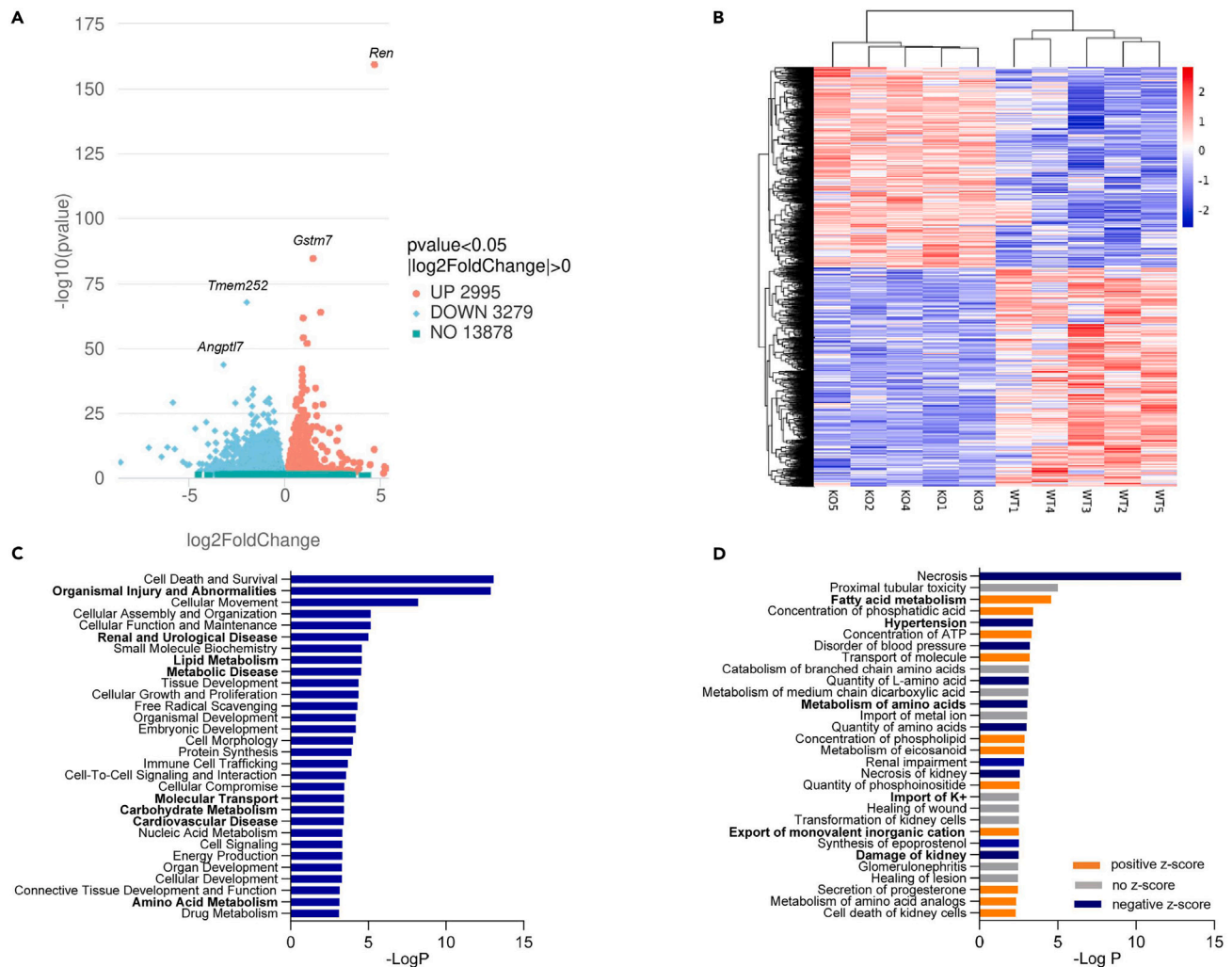https://doi.org/10.1016/j.isci.2024.110901

Figure 1. Top significantly changed diseases and functions in KO rats

(A) Volcano plot of gene expression level. Each dot represents one gene. The red, blue, and green colors indicate genes that are significantly upregulated, downregulated and not significantly changed, respectively. The significance level was determined as $p < 0.05$ ($-\log p > 1.3$).

(B) Clustering heatmap of differentially expressed genes in KO rats compared to WT rats.

(C) Top 30 significantly altered categories of diseases and functions in KO rats based on ingenuity pathway analysis (IPA). Significance level was determined as $p < 0.05$ ($-\log p > 1.3$).

(D) Top 30 significantly altered diseases and functions based on the highlighted categories in KO rats predicted by IPA. The significance level was determined as $p < 0.05$ ($-\log p > 1.3$). Positive and negative Z score indicates the prediction of activation and suppression of diseases and functions, respectively. No Z score indicates that IPA could not predict the activation or suppression of the diseases and functions based on the related gene change profile.

RESULTS

Deletion of *Kcnj16* significantly altered the gene expression level of SS rats

To identify genes and pathways differentially expressed between WT and KO rats, we performed RNA sequencing (RNA-seq) on the kidney cortex tissue of WT and KO rats. Transcriptomic analysis indicated that deletion of *Kcnj16* significantly altered the gene expression levels of SS rats with over 6,000 significantly changed genes, with *Ren* (the gene encoding renin) being the most upregulated gene (Figures 1A and 1B). Our previous studies revealed that KO rats exhibited an alteration in the renin-angiotensin-aldosterone system,[13] which is consistent with the current observation. The top 30 significantly changed categories of diseases and functions based on ingenuity pathway analysis (IPA) indicated that deletion of *Kcnj16* altered genes related to renal and cardiovascular diseases, metabolic processes, and molecular transport (Figure 1C). To further look at the specific diseases and functions within the categories that are mostly correlated with the phenotype of the KO rats (highlighted in Figure 1C), IPA predicted reduced kidney damage, blood pressure, and amino acid metabolism, while activated ion transport and fatty acid metabolism upon deletion of *Kcnj16* (Figure 1D).
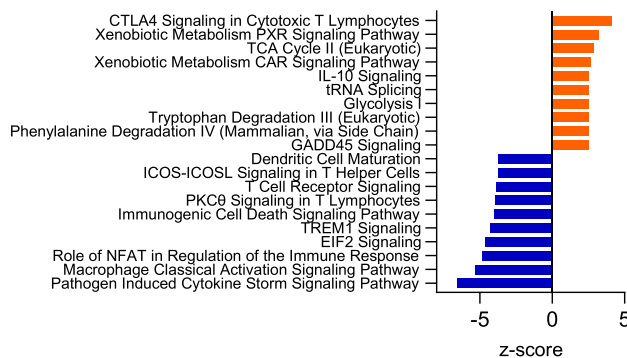
Figure 2. Top 10 up- and downregulated canonical pathways in KO rats
The significance level was determined as $p < 0.05$ ($-\log p > 1.3$). The pathways were chosen based on their Z score.

Canonical pathway analysis suggests activation of metabolic-related pathways while inhibition of immune response-related pathways in KO rats

Subsequently, we analyzed the significantly changed canonical pathways in the absence of *Kcnj16*. The top 10 up- and downregulated canonical pathways in KO rats predicted by IPA suggested activation of metabolic-related pathways (e.g., xenobiotic metabolism, tricarboxylic acid [TCA] cycle, phenylalanine degradation, etc.) and inhibition of immune response-related pathways (e.g., pathogen-induced cytokine storm signaling pathway, macrophage classical activation signaling pathway, nuclear factor of activated T cells pathway, etc.) (Figure 2).

Significantly changed genes related to reduced hypertension and kidney damage

We further analyzed the differentially expressed genes related to altered diseases, functions, and canonical pathways. IPA suggested a large number of differentially expressed genes that are related to the inhibition of hypertension and kidney damage (Figure 3; Tables S1 and S2). There were 39 differentially expressed genes that are predicted to inhibit hypertension (Figure 3A; Table S1), with most of them being enzymes (e.g., *Nlrp3* and *Nos3*), growth factors (e.g., *Pdgfd* and *Vegfa*), and ion channels (e.g., *Kcnj8* and *Trpv4*). On the other hand, 47 significantly changed genes are predicted to reduce kidney damage (Figure 3B; Table S2), with most of them being inflammatory-related genes (e.g., *Il18*, *Cxcr3*, *Tlr4*, etc.). The top differentially expressed genes are also validated by qPCR and immunohistochemistry (Figures S1 and S2). In addition, fragments per kilobase of transcript per million mapped reads analysis of the inflammatory cytokines and receptors that are related to the development of SS hypertension and renal damage indicated a significant decrease of *Il1b* (IL-1β), *Ifngr1* (IFN-γ1), *Il17ra* (1L-17 receptor A), and *Il17rb* (IL-17 receptor B) (Figure 3C). Based on the differentially expressed genes, IPA also identified 54 significantly related (p value of overlap <0.05) upstream regulators (Table S3). Among them, multiple genes were associated with SS hypertension (e.g., *Nox4*, *Nfat5*, and *Ppp3r1*) and inflammation (e.g., *Nfkb1*, *p38-mapk*, and *Il4*).

Significantly changed genes related to disturbed ion transport

Since deletion of *Kcnj16* caused severe hypokalemia and salt-wasting phenotype in SS rats,[3] we also analyzed the genes related to K$^+$, Na$^+$, Ca^{2+}, and Cl$^-$ transport. Results indicated that compared to WT rats, KO rats have increased transport of Na$^+$, Ca^{2+}, and Cl$^-$, while transport of K$^+$ was inhibited (Tables 1, 2, 3, and 4). For K$^+$ transport, multiple potassium channels in inwardly rectifying potassium channel subfamily J (KCNJ, encoded by *Kcnj* genes, e.g., *Kcnj1*) and the voltage-gated potassium channel subfamily Q (KCNQ, encoded by *Kcnq* genes, e.g., *Kcnq3*) were significantly altered, as well as a significant increase of the WNK (*Wnk4*)-SPAK (*Stk39*)-NCC (*Slc12a3*) pathway[23,24] (Table 1). For Na$^+$ transport, there was a significantly increased expression of the genes encoding the α, β, and γ subunits of the epithelial sodium channel (ENaC, encoded by *Scnn1a*, *Scnn1b*, and *Scnn1g*), as well as multiple solute carrier (SLC, encoded by *Slc* genes, e.g., *Slc12a2*) transporters (Table 2). For Ca^{2+} transport, various genes of calcium voltage-gated channel subunits (CACN, encoded by *Cacn* genes, e.g., *Cacnb2*) and transient receptor potential (TRP, encoded by *Trp* genes, e.g., *Trpc3*) channels were significantly changed (Table 3). For Cl$^-$ transport, there was a significantly decreased expression of pendrin (*Slc26a4*) while significantly increased expression of genes of voltage-gated chloride (CLCN, encoded by *Clcn* genes, e.g., *Clcn6*) channels and intracellular chloride (CLIC, encoded by *Clic* genes, e.g., *Clic3*) channels (Table 4).

Deletion of *Kcnj16* significantly altered the metabolic profile in SS rats

Untargeted metabolomic analysis identified 219, 790, and 31 differentially expressed metabolites in plasma, urine, and kidney in KO rats compared to WT rats (Figures 4A–4C). Orthogonal projections to latent structures discriminant analysis indicated apparent differences between the metabolic profile of plasma, urine, and kidney of WT and KO rats (Figures 4D–4F).
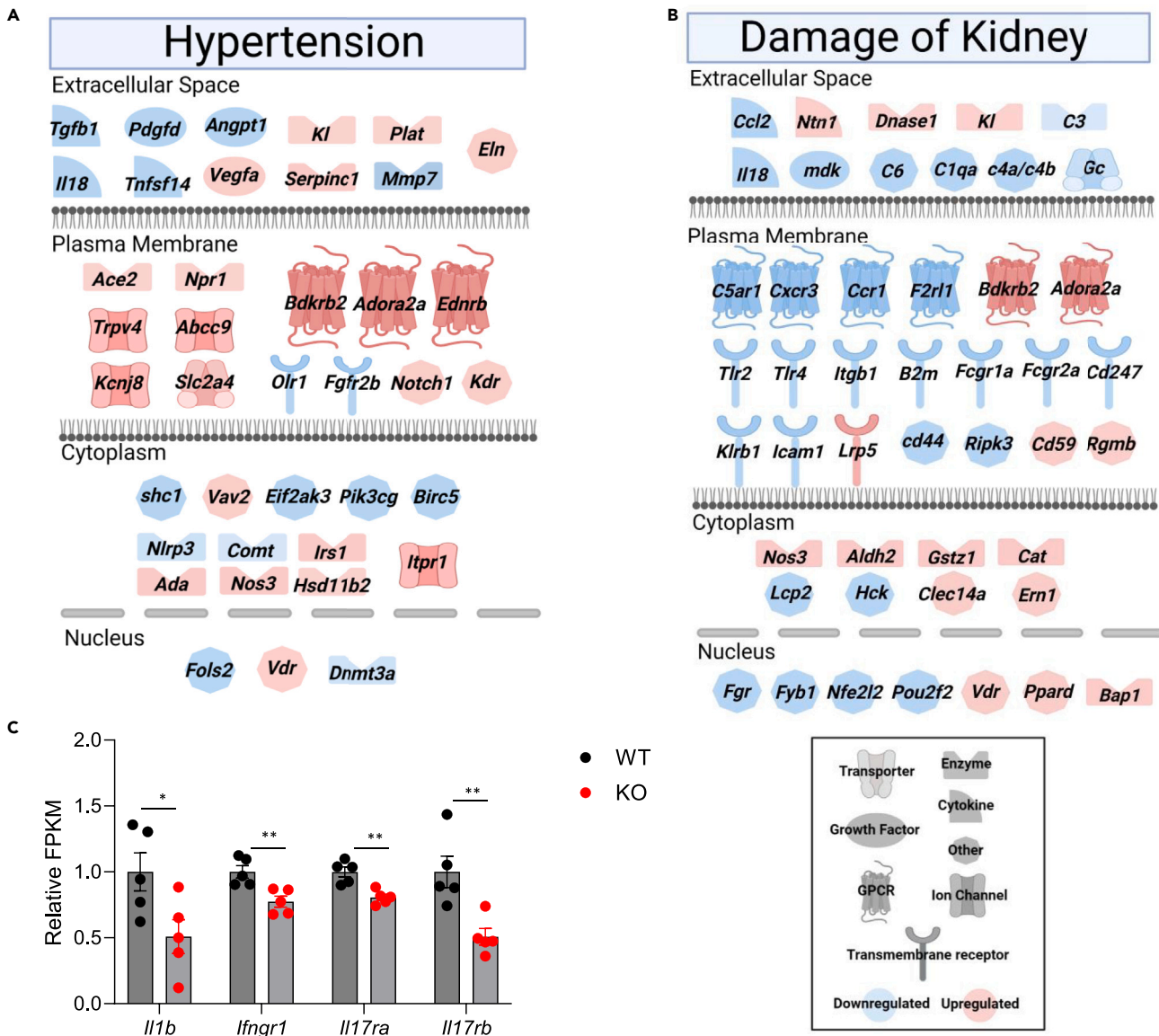
Figure 3. Significantly changed genes related to inhibition of hypertension and kidney damage

(A) Significantly changed genes related to inhibition of hypertension.

(B) Significantly changed genes related to inhibition of kidney damage.

(A and B) were modified from IPA. Only genes that are predicted to inhibit hypertension or kidney damage are shown here. A complete list of genes that are related to hypertension and kidney damage is shown in Tables S1 and S2. Significance level was determined as $p < 0.05$ ($-\log p > 1.3$).

(C) Relative fragments per kilobase of transcript per million mapped reads (FPKM) expression of differentially expressed inflammatory cytokines and receptors related to the development of SS hypertension and kidney damage. Data were normalized to the FPKM of WT rats. Data are represented as mean $\pm$ SEM. The significance level was determined by the Student's t test. $*p < 0.05$, $**p < 0.01$.

Significantly altered diseases and functions and canonical pathways in plasma, urine, and kidney of KO rats based on untargeted metabolomic analysis

IPA based on the differentially expressed metabolites in plasma, urine, and kidney revealed changes in multiple diseases and function categories (Figures 5A–5C). Some common diseases and functions include organismal injury and abnormalities, carbohydrate metabolism, lipid metabolism, amino acid metabolism, etc. Renal and urological system development and function and cardiovascular disease were also identified in the plasma (Figure 5A). For the significantly changed canonical pathways, spermine and spermidine degradation (the use of acetyl-CoA to convert spermine and spermidine to N^1-acetylated derivatives in the cytosol)[25] was identified in both plasma and urine, while taurine biosynthesis was identified in both urine and kidney (Figures 5D–5F).

Table 1. Differentially expressed genes related to the transport of K⁺

Symbol	Ensembl/Entrez Gene/GenBank/Gene Symbol - rat (Entrez Gene)	Expr log ratio	Expr p value
Calm1 (includes others)	ENSRNOG00000004060	−0.40	1.01E−13
Kcnk3	ENSRNOG00000009790	1.93	1.04E−10
Gja5	ENSRNOG00000017484	1.01	1.51E−10
Kcnk2	ENSRNOG00000002653	2.19	3.01E−09
Dpp6	ENSRNOG00000030547	−0.62	2.02E−05
Atp1a4	ENSRNOG00000032378	−1.37	2.21E−05
Kcna5	ENSRNOG00000019719	1.65	5.16E−05
Nos3	ENSRNOG00000009348	0.49	7.02E−05
Abcc9	ENSRNOG00000036960	0.63	9.09E−05
Kcnk1	ENSRNOG00000019937	−0.49	3.06E−04
Kcnc4	ENSRNOG00000060988	0.70	4.48E−04
Slc12a6	ENSRNOG00000005196	0.25	6.08E−04
Adora1	ENSRNOG00000003442	−1.07	6.98E−04
Kcnn4	ENSRNOG00000019440	−1.08	8.72E−04
Wnk4	ENSRNOG00065033320	0.37	9.80E−04
Atp1a1	ENSRNOG00000030019	0.34	1.47E−03
Kcnj8	ENSRNOG00000013463	0.66	1.71E−03
Stk39	ENSRNOG00000024808	0.45	2.04E−03
Kcnj15	Kcnj15	0.29	2.96E−03
Kcns3	ENSRNOG00000004899	−0.79	2.96E−03
Slc12a2	ENSRNOG00000015971	0.22	3.13E−03
Tmem38a	ENSRNOG00000011912	0.51	5.34E−03
Kcnj11	ENSRNOG00000021128	−1.53	6.95E−03
Tmem175	ENSRNOG00000000044	0.28	7.31E−03
Kcnmb2	ENSRNOG00000010094	1.94	7.98E−03
Kcnj3	ENSRNOG00000005369	−0.93	8.94E−03
Pkd2	ENSRNOG00000002146	0.17	9.12E−03
Kcnb1	ENSRNOG00000046949	−0.35	1.07E−02
Hpn	ENSRNOG00000021097	0.32	1.21E−02
Kcnq1	ENSRNOG00000020532	0.40	1.69E−02
Kcng2	ENSRNOG00000053640	0.62	2.27E−02
Kcnt1	ENSRNOG00000017283	0.50	2.60E−02
Edn3	ENSRNOG00000007477	−1.01	3.21E−02
Kcnj10	ENSRNOG00000068444	0.47	3.22E−02
Aqp1	ENSRNOG00000011648	0.16	4.05E−02
Kcnq3	ENSRNOG00000005206	2.78	4.13E−02
Kcnj1	ENSRNOG00000059005	0.36	4.65E−02

Upstream regulators based on the changes in the metabolomic profile

Upstream analysis based on the changes of the metabolomic profile in plasma, urine, and kidney revealed multiple overlapping regulators (Figure 6; Table S4). *Slc6a12* (betaine-GABA transporter, BGT1), L-cysteine, and betaine were commonly identified for plasma and kidney. Agmatine was identified for both plasma and urine. A complete list of upstream regulators is shown in Table S4. For the upstream regulators that are chemicals, only endogenous mammalian chemicals are chosen (chemical drugs and toxicants are excluded).

Integration of transcriptomic and metabolomics analysis

Based on the integration analysis of differentially expressed genes and metabolites, we identified alterations in the TCA cycle, amino acid metabolism, and reactive oxygen species (ROS) metabolism that are related to SS hypertension (Figure 7). Transcriptomic analysis suggested

Table 2. Differentially expressed genes related to the transport of Na⁺

Symbol	Ensembl/Entrez Gene/GenBank/Gene Symbol - rat (Entrez Gene)	Expr log ratio	Expr p value
Ano6	ENSRNOG00000006995	0.23	1.25E−03
Atp1a1	ENSRNOG00000030019	0.34	1.47E−03
Atp1a4	ENSRNOG00000032378	−1.37	2.21E−05
Cftr	ENSRNOG00000055103	−2.47	4.76E−11
Chp2	ENSRNOG00000019112	−1.41	2.06E−02
Cnksr3	ENSRNOG00000018052	−0.26	3.70E−02
Cntfr	ENSRNOG00000047307	1.65	4.70E−18
Cntn1	ENSRNOG00000004438	−4.48	3.90E−05
Cyp2c23	ENSRNOG00000013291	0.49	1.28E−10
Dmpk	ENSRNOG00000015085	0.39	1.39E−03
Egf	ENSRNOG00000053979	0.81	2.29E−02
Fgf13	ENSRNOG00000042753	−0.50	9.75E−05
Gnas	ENSRNOG00000047374	0.21	4.82E−03
Gpd1l	ENSRNOG00000026455	0.19	2.91E−02
Il1b	ENSRNOG00000004649	−0.98	3.64E−02
Kcnk1	ENSRNOG00000019937	−0.49	3.06E−04
Kcnq1	ENSRNOG00000020532	0.40	1.69E−02
Mapkap1	ENSRNOG00000017583	0.31	7.27E−03
Ndrg2	ENSRNOG00000010389	1.11	1.48E−31
Nedd4	ENSRNOG00000058898	−0.15	5.60E−03
Nos3	ENSRNOG00000009348	0.49	7.02E−05
Pkd2	ENSRNOG00000002146	0.17	9.12E−03
Scn7a	ENSRNOG00000029342	0.90	2.40E−02
Scn8a	ENSRNOG00000005309	−1.11	1.54E−05
Scnn1a	ENSRNOG00000019368	0.47	1.76E−02
Scnn1b	ENSRNOG00000030981	0.35	1.91E−04
Scnn1g	ENSRNOG00000017842	0.44	1.71E−03
Sgk1	ENSRNOG00000011815	1.35	3.64E−04
Slc12a2	ENSRNOG00000015971	0.22	3.13E−03
Slc12a3	ENSRNOG00000057072	0.50	4.10E−04
Slc13a3	ENSRNOG00000019118	0.38	3.11E−06
Slc17a2	ENSRNOG00000017180	0.31	4.22E−03
Slc17a3	ENSRNOG00000032745	0.60	2.33E−11
Slc17a4	ENSRNOG00000022505	0.56	4.76E−08
Slc23a2	ENSRNOG00000021262	0.25	9.25E−04
Slc34a1	ENSRNOG00000015262	0.40	1.27E−04
Slc34a3	ENSRNOG00000010451	0.29	6.28E−03
Slc38a7	ENSRNOG00000012007	0.21	7.52E−03
Slc4a4	ENSRNOG00000003134	0.21	2.57E−02
Slc9a2	ENSRNOG00000015567	0.59	2.39E−05
Slc9a3	ENSRNOG00000015159	0.48	1.88E−04
Stk39	ENSRNOG00000024808	0.45	2.04E−03
Tgfb1	ENSRNOG00000020652	−0.57	7.12E−04
Tpcn1	ENSRNOG00000059344	0.52	6.17E−19
Wnk4	ENSRNOG00065033320	0.37	9.80E−04
Ywhah	ENSRNOG00000055471	−0.55	1.84E−06

Table 3. Differentially expressed genes related to the transport of Ca²⁺

Symbol	Ensembl/Entrez Gene/GenBank/Gene Symbol - rat (Entrez Gene)	Expr log ratio	Expr p value
Ano6	ENSRNOG00000006995	0.23	1.25E−03
Atp2a3	ENSRNOG00000017912	0.71	2.90E−08
Cacna1a	ENSRNOG00000052707	0.53	9.13E−04
Cacna1g	ENSRNOG00000060528	0.61	1.12E−02
Cacna1h	ENSRNOG00000033893	−1.12	5.21E−03
Cacnb2	ENSRNOG00000018378	0.76	8.80E−03
Cacnb3	ENSRNOG00000054274	−0.90	1.24E−02
Calb1	ENSRNOG00000007456	−1.22	8.19E−03
Camk2b	ENSRNOG00000052080	−1.62	5.29E−03
Ccr1	ENSRNOG00000086224	−2.01	2.21E−03
Ccr5	ENSRNOG00000049115	−0.82	3.11E−04
Coro1a	ENSRNOG00000019430	−0.82	1.01E−05
Cxcl12	ENSRNOG00000013589	−0.73	2.67E−10
Cysltr1	ENSRNOG00000037845	−1.55	7.29E−03
Dnm1l	ENSRNOG00000001813	−0.20	1.48E−02
Edn1	ENSRNOG00000014361	−1.06	3.32E−04
Ednrb	ENSRNOG00000010997	0.44	2.54E−05
Egf	ENSRNOG00000053979	0.81	2.29E−02
F2	ENSRNOG00000016325	0.49	1.06E−02
F2rl1	ENSRNOG00000018003	−0.70	2.67E−04
Gja1	ENSRNOG00000000805	−1.16	1.03E−04
Itgav	ENSRNOG00000004912	−0.25	3.02E−02
Itpr1	ENSRNOG00000007104	0.32	1.31E−04
Kcnj8	ENSRNOG00000013463	0.66	1.71E−03
Kcnn4	ENSRNOG00000019440	−1.08	8.72E−04
Klk1	ENSRNOG00000068378	4.64	7.27E−10
Mcoln1	ENSRNOG00000000975	0.23	5.88E−04
Mcoln3	ENSRNOG00000015024	−0.59	1.00E−03
Mcub	ENSRNOG00000009433	1.54	2.24E−03
Nos3	ENSRNOG00000009348	0.49	7.02E−05
P2ry12	ENSRNOG00000013902	−1.11	1.46E−03
Pdzd11	Pdzd11	−0.20	4.69E−02
Pkd1	ENSRNOG00000010771	0.24	6.23E−03
Pkd2	ENSRNOG00000002146	0.17	9.12E−03
Plcb2	ENSRNOG00000058337	−1.36	7.24E−05
Ppp1r1a	ENSRNOG00000036827	0.45	4.46E−03
Prlr	ENSRNOG00000057557	−1.09	1.16E−04
Pth1r	ENSRNOG00000020948	0.35	1.31E−06
Ramp1	ENSRNOG00000019926	−1.61	4.47E−04
Ramp3	ENSRNOG00000053766	0.49	1.84E−03
Ryr2	ENSRNOG00000017060	−1.00	9.35E−03
Selenok	ENSRNOG00000014624	−0.35	1.15E−05
Smdt1	Smdt1	0.22	4.27E−03
Tmc1	ENSRNOG00000051262	1.44	3.88E−02
Tmco1	ENSRNOG00000003928	−0.26	2.47E−02

Table 3. Continued

Symbol	Ensembl/Entrez Gene/GenBank/Gene Symbol - rat (Entrez Gene)	Expr log ratio	Expr p value
Tmem165	ENSRNOG00000002199	−0.19	4.19E−02
Trpc3	ENSRNOG00000016070	1.05	1.71E−09
Trpc4ap	ENSRNOG00000019152	0.32	3.21E−04
Trpm6	ENSRNOG00000013053	0.40	1.66E−03
Trpv4	ENSRNOG00000001195	0.36	8.03E−04
Trpv5	ENSRNOG00000015394	−0.78	2.06E−05
Trpv6	ENSRNOG00000014714	−0.86	4.57E−02
Vdr	ENSRNOG00000054420	0.24	1.82E−02
Wdr37	ENSRNOG00000016834	0.33	2.37E−05

elevated expression of nearly all enzymes in the TCA cycle, especially fumarase (*Fh*), where metabolomics suggests the significant increase of L-arginine in the kidney of KO rats (Figure 7A). For amino acid metabolism, besides L-arginine, both transcriptomic and metabolomic analyses suggested alteration of the quantity of taurine in KO rats, with taurine significantly increased in plasma while decreased in the kidney (Figure 7B). For ROS metabolism, both transcriptomics and metabolomics data suggested decreased generation and quantity of ROS, which was indicated by multiple related genes like *Tgfb1*, as well as the increased amount of L-arginine in the kidney (Figure 7C).

DISCUSSION

The essential role of $K_{ir}5.1$ in renal salt handling and blood pressure control has been demonstrated in both human and animal models.[3,5,8,26] However, the underlying mechanisms are still not fully understood. Here, we used an integration of transcriptomic and metabolomic analysis to provide more insights into the effect of $K_{ir}5.1$ in SS hypertension.

Table 4. Differentially expressed genes related to the transport of Cl⁻

| Symbol	Ensembl/Entrez Gene/GenBank/Gene Symbol - rat (Entrez Gene)	Expr log ratio	Expr p value
Slc26a4	ENSRNOG00000058692	−1.03	4.60E−16
Clcn4	ENSRNOG00000003533	0.51	3.16E−11
Cftr	ENSRNOG00000055103	−2.47	4.76E−11
Slc4a1	ENSRNOG00000020951	0.80	4.96E−11
Clcnka	ENSRNOG00000009897	0.62	1.13E−08
Slc5a8	ENSRNOG00000006367	−0.76	2.64E−07
Slc1a1	ENSRNOG00000014816	0.42	1.62E−06
Clic1	ENSRNOG00000029682	−0.48	2.52E−06
Bsnd	ENSRNOG00000006543	0.46	6.75E−05
Clic3	ENSRNOG00000015184	0.54	7.21E−05
Ano1	ENSRNOG00000020865	0.70	1.29E−04
Slc12a3	ENSRNOG00000057072	0.50	4.10E−04
Tgfb1	ENSRNOG00000020652	−0.57	7.12E−04
P2ry6	ENSRNOG00000019270	−0.80	8.59E−04
Wnk4	ENSRNOG00065033320	0.37	9.80E−04
Ano6	ENSRNOG00000006995	0.23	1.25E−03
Slc12a2	ENSRNOG00000015971	0.22	3.13E−03
Bdnf	ENSRNOG00000047466	−2.29	4.43E−03
Clic5	ENSRNOG00000047218	0.21	1.16E−02
Ostm1	ENSRNOG00000037647	0.26	1.25E−02
Ada	ENSRNOG00000010265	0.40	1.80E−02
Clcn6	ENSRNOG00000008345	0.27	2.60E−02
Slc26a2	ENSRNOG00000018082	−0.39	4.03E−02
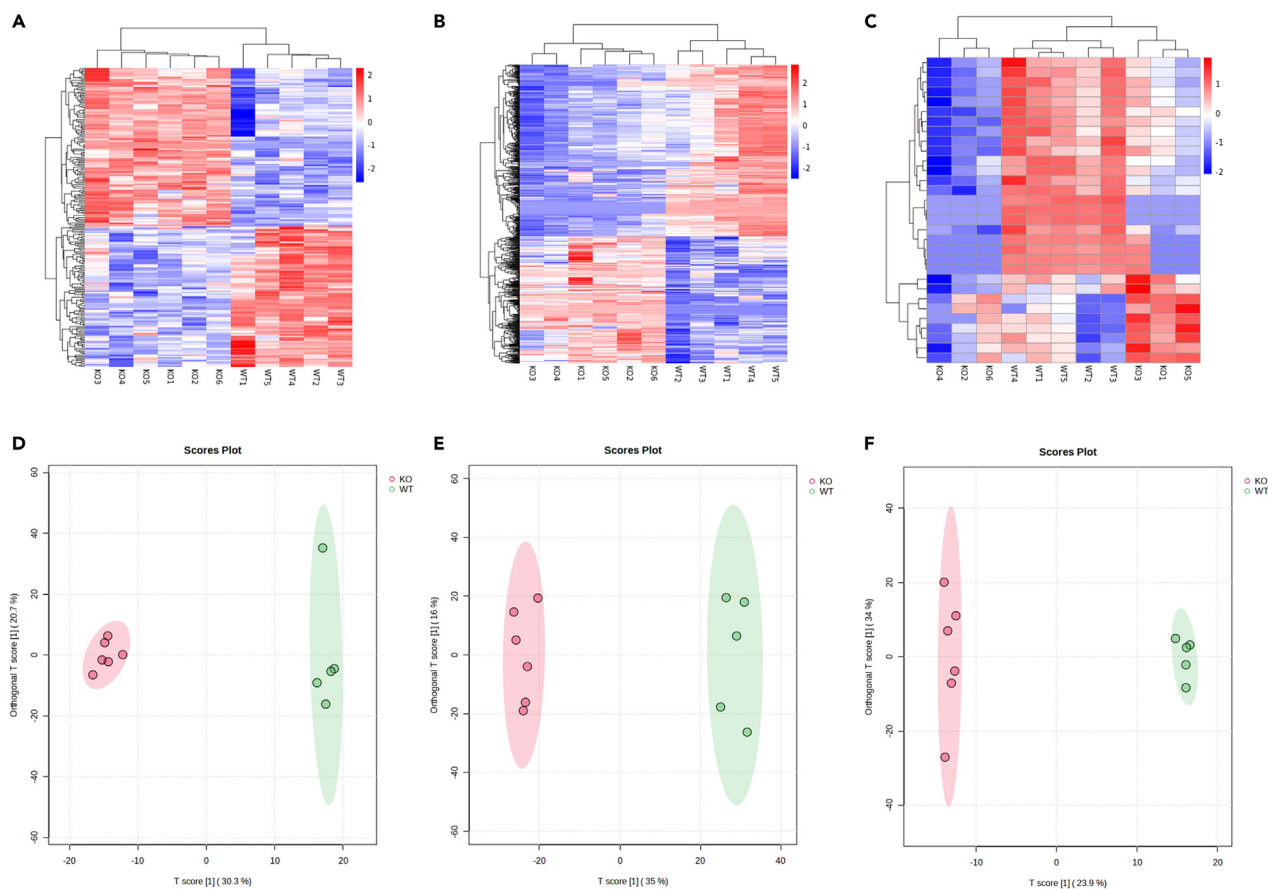
Figure 4. Differentially expressed metabolites in plasma, urine, and kidney of SS$^{Kcnj16-/-}$ rats

(A–C) Clustering heatmap of differentially expressed metabolites in plasma (A), urine (B), and kidney (C) of KO rats compared to WT rats. The significance level was determined as *p adjusted* <0.05.

(D–F) Orthogonal projections to latent structures discriminant analysis (OPLS-DA) of metabolites in plasma (D), urine (E), and kidney (F) of WT and KO rats.

Consistent with the phenotype observed in KO rats,[3] transcriptomic profiling suggests that deletion of $K_{ir}5.1$ reduced blood pressure and kidney damage and shifted ion transport activities in SS rats (Figure 1). Interestingly, although both the phenotype and transcriptomics profiling indicate reduced kidney damage in the KO rats, further high salt (4%) challenge triggers mortality of the rats, which we suspect is most likely due to severe hypokalemia, as supplementation of the high-salt diet with potassium not only rescues these rats from salt-induced mortality but also keeps their blood pressure at the normal level.[3]

Surprisingly, besides the differential expression of genes related to ion transport (Figure 1; Tables 1, 2, 3, and 4), canonical pathway analysis using IPA suggests significant downregulation of immune response-related pathways while upregulation of metabolic-related pathways (Figure 2). The essential role of immune cells in SS hypertension and renal damage has been demonstrated by various studies in recent years.[27–30] Studies using both animal models and cultured human monocytes demonstrated that Na$^+$ can enter the antigen-presenting cells (APCs) like dendritic cells (DCs) through the ENaC to trigger protein kinase C- and serum/glucocorticoid kinase-1-stimulated activation of nicotinamide adenine dinucleotide phosphate oxidase (NAPDH), which can increase the production of pro-inflammatory cytokines like IL-1β, IL-6, etc., by DCs. These cytokines will further polarize IL-17-producing T cells to induce vascular inflammation, enhance renal Na$^+$ reabsorption, and ultimately lead to hypertension.[30–32] Consistent with these findings, our canonical pathway analysis suggests suppressed T cell receptor signaling and DC maturation in KO rats, which might have protective effects against SS hypertension (Figure 2). On the other hand, gene expression analysis also revealed a significantly decreased expression of *Il1b* (IL-1β), *Ifngr1* (IFN-γ1), *Il17ra* (1L-17 receptor A), and *Il17rb* (IL-17 receptor B) in KO rats, which may mimic the situation where genetic deletion and/or pharmacological blockade of inflammatory cytokines attenuate hypertension[33] (Figure 3C). We also observed a significant decrease of other inflammatory-related genes like *Nlrp3*, *Tlr2*, *Tlr4*, etc., which have also been shown to reduce pressure and renal damage in SS hypertension upon inhibition[34,35] (Figures 3A and 3B; Table S2). Additionally, upstream analysis indicates a significant decrease in the NF-κB (*Nfkb*) complex, which can also attenuate SS hypertension[36] (Table S3). Considering the severely altered electrolyte transport in the KO rats (Tables 1, 2, 3, and 4), the decreased immune responses may be due to the reduced amount of
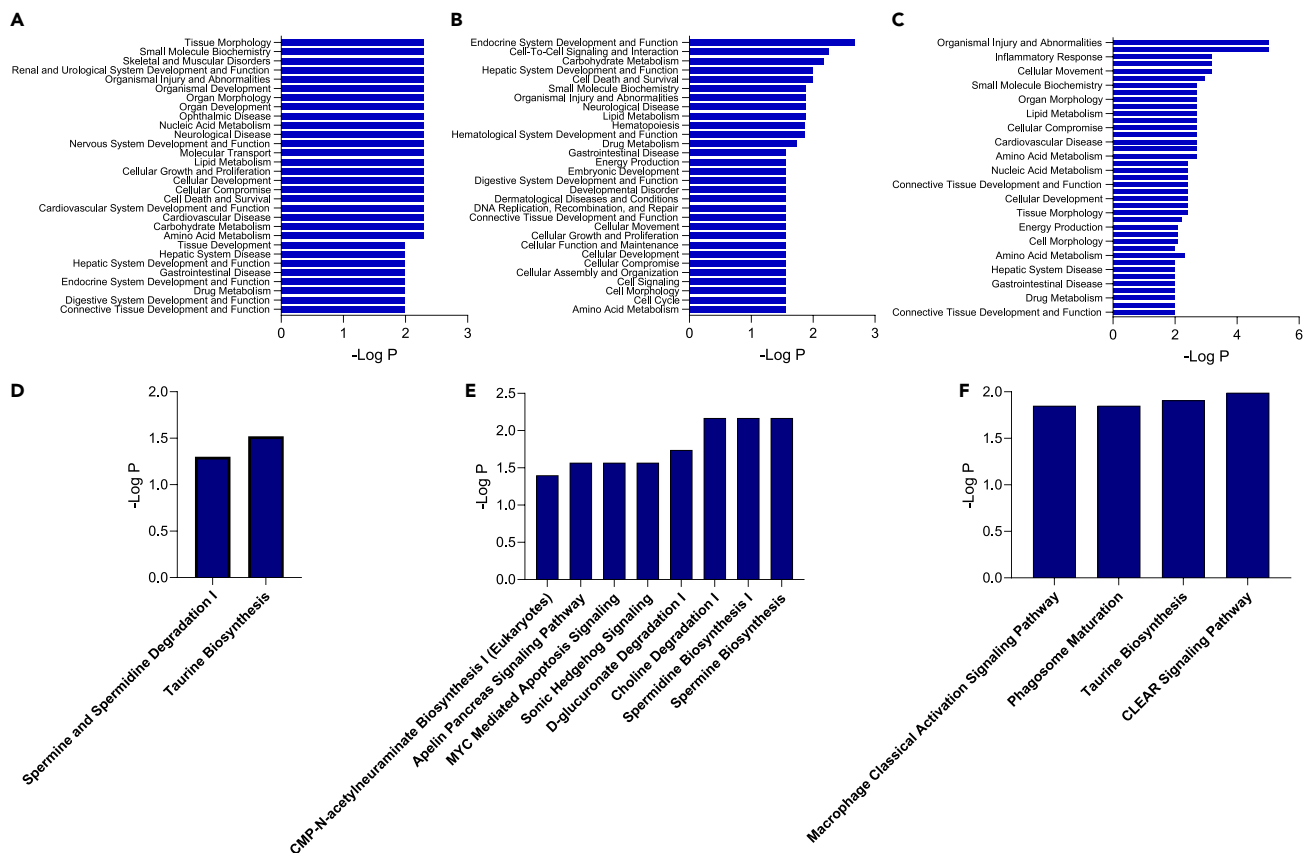
Figure 5. Significantly changed diseases, functions, and canonical pathways in plasma, urine, and kidney of KO rats based on the untargeted metabolomic analysis

(A–C) Top 30 significantly changed diseases and function categories in plasma (A), urine (B), and kidney (C) of KO rats based on the *p* value.

(D–F) Significantly changed canonical pathways in plasma (D), urine (E), and kidney (F) of KO rats. Significance level was determined as *p* < 0.05 (−log *p* > 1.3).

Na$^+$ that enters the APCs compared to WT rats, which may attenuate the activation of APCs and downstream immune responses and ultimately attenuates the elevation of blood pressure.

Numerous studies in both human and animal models have demonstrated a positive correlation between metabolic profile and hypertension.[37–41] Similar to transcriptomic analysis, our untargeted metabolomic analysis also suggests distinct metabolic profiles of urine, plasma, and kidney between WT and KO rats with similar altered diseases and functions like organism injury and abnormalities, amino acid metabolism, etc. (Figures 4 and 5). Interestingly, all overlapped upstream regulators for the metabolomics profile, L-cysteine, agmatine, and betaine are related to hypertension (Figure 6).[42–45] To further look at the metabolomic pathways in the kidney that are associated with SS hypertension, the integration of transcriptomics and metabolomics analysis identified multiple genes and metabolites related to the alteration of the TCA cycle, amino acid metabolism, and ROS metabolism in SS rats lacking K$_{ir}$5.1 (Figure 7).[37]

TCA cycle

Previous proteomic analysis suggests that overexpression of fumarase in SS rats attenuates SS hypertension, while knockdown of fumarase exacerbates salt-induced hypertension in Sprague-Dawley rats.[46–48] Our canonical pathway analysis suggested an activated TCA cycle in KO rats with a significantly increased expression of multiple enzymes in the TCA cycle, including fumarase (*Fh*), which can attenuate the elevation of blood pressure through increased L-arginine.[47] Consistently, L-arginine was also significantly increased in the kidney tissue of KO rats as detected by metabolomic analysis (Figure 7A). In addition, our transcriptomics data also indicated an increased expression of succinate dehydrogenase (*Sdha*, *Sdhc*), which may mitigate the blood pressure development through decreasing succinate, as an increased amount of succinate is associated with the elevation of blood pressure[49] (Figure 7A).

Amino acid metabolism

The anti-hypertensive effect of L-arginine through the enhancement of nitric oxide (NO) production has been demonstrated by numerous studies.[50,51] Besides L-arginine, both transcriptomics and metabolomics analyses suggest changes in the amount of L-taurine in the KO
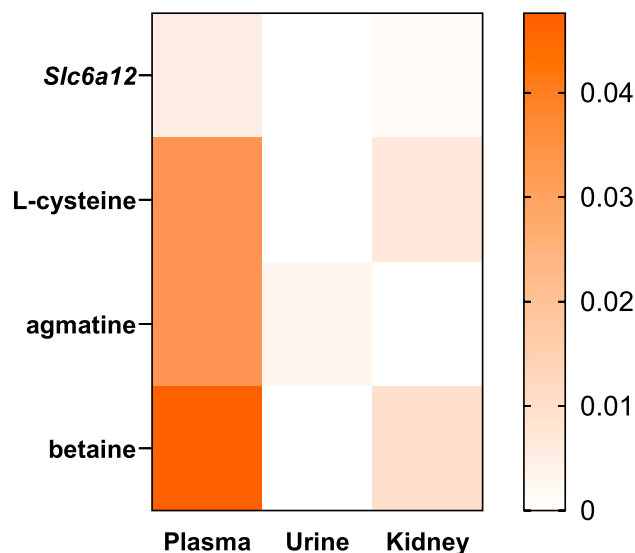
Figure 6. Overlapped upstream regulators for the metabolic profile of plasma, urine, and kidney

A complete list of upstream regulators is listed in Table S4. For the upstream regulators that are chemicals, only endogenous mammalian chemicals are chosen (chemical drugs and toxins are excluded). Significance level was determined as $p < 0.05$ ($-\log p > 1.3$).

rats (Figure 7B). Taurine, which was recently reported as the metabolite associated with aging and adverse health, such as hypertension, inflammation, and prevalence of type 2 diabetes,[52] was also significantly altered between WT and KO rats. Previous study has shown that taurine supplementation significantly increased plasma taurine concentrations and decreased blood pressure in prehypertensive individual, with further mechanistic study suggesting that taurine treatment upregulates the expression of hydrogen sulfide-synthesizing enzymes and reduces agonist-induced vascular reactivity through the transient receptor potential channel subtype 3-mediated calcium influx in human and mouse mesenteric arteries.[53] The increased amount of taurine in the plasma of KO rats likely attenuates the blood pressure through a similar mechanism (Figure 7B). This is also consistent with the upstream regulating effects of L-cysteine (Figure 6), which not only affects taurine but also influences the homeostasis of glutathione and glutathione disulfide to reduce hypertension.[44]

ROS metabolism

Multiple studies have suggested a correlation between high salt intake, increased ROS, and hypertension.[35,54,55] ROS, such as superoxide anion, hydrogen peroxide, and hydroxyl anion, are reactive byproducts of mitochondrial respiration or oxidases, NADPH oxidase, xanthine oxidoreductase, and certain arachidonic acid oxygenase.[56,57] In the kidney, increased production of ROS can initiate hypertension through multiple mechanisms, e.g., increasing renal vasoconstriction, renin release, etc.[57] Based on our transcriptomics data, IPA predicted decreased generation and quantity of ROS in the kidney of KO rats, which is consistent with the reduced blood pressure phenotype (Figure 7C). Consistently, the metabolomics results suggest increased amount of L-arginine, which can enhance NO production and reduce ROS.[58] The decreased ROS also aligns with the decreased *Il17ra and Il17rb*, where IL-17 has been suggested to promote inflammation through the generation of ROS.[59]

In conclusion, the integrated transcriptomic and metabolomic analysis revealed that besides altered ion transport, the decreased blood pressure and renal damage in the absence of $K_{ir}5.1$ in Dahl SS rats might also be due to decreased inflammation, altered TCA cycle, and amino acid and ROS metabolism, which provides comprehensive insights into the essential role of $K_{ir}5.1$ in SS hypertension.

Limitations of the study

There are several limitations of the study. Firstly, the current study mainly focused on the SS hypertension by using Dahl SS rats; further studies are needed to examine the effect of *Kcnj16* in normal salt-resistant rats. Secondly, the *Kcnj16* KO rat model used in this study is a global knockout, so although we used renal cortex tissue for bulk RNA-seq, the observed changes in genes are still possibly due to the lack of *Kcnj16* in other organs. Further studies may use kidney-specific *Kcnj16* KO animal models to specifically look at how renal *Kcnj16* affects transcriptomic and metabolomic profiles. Thirdly, we performed bulk RNA-seq in this study, which cannot reveal the gene changes in specific tubule segments. Further studies may use single-cell RNA-seq to investigate how deletion of *Kcnj16* affects the gene expressions along different renal tubule segments. Additionally, this study only used male rats; further studies on female rats might provide more comprehensive insights. Finally, although the proposed pathways predicted by transcriptomics and metabolomics analyses provide insights for potential mechanisms into the role of $K_{ir}5.1$ in SS hypertension, follow-up studies, e.g., pharmacological inhibition of specific pathways, are needed to sufficiently validate the conclusion.
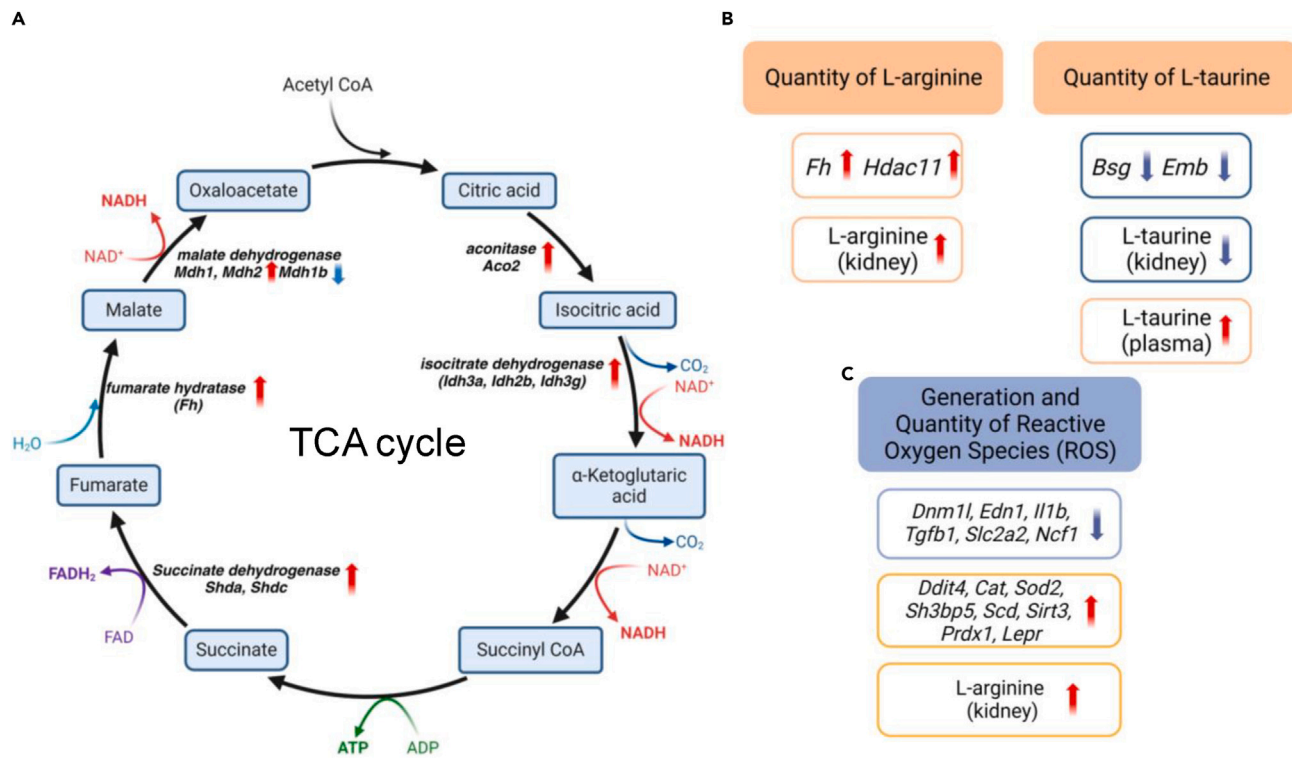
Figure 7. Integration of transcriptomics and metabolomics analysis

(A) Significantly changed genes in TCA cycle.

(B) Significantly changed genes and metabolites related to increased amounts of L-arginine and L-taurine in KO rats.

(C) Significantly changed genes and metabolites related to decreased generation and quantity of reactive oxygen species (ROS) in KO rats. For metabolites, the significance level was determined as *p adjusted* <0.05. For genes, the significance level was determined as $p < 0.05$ ($-\log p > 1.3$).

RESOURCE AVAILABILITY

Lead contact

Further information and requests for resources and reagents should be directed to and will be fulfilled by the lead contact, Dr. Alexander Staruschenko (staruschenko@usf.edu).

Materials availability

This study did not generate new unique reagents or animal models.

Data and code availability

- RNA-seq data are publicly available through Gene Expression Omnibus (GEO): GSE244052; https://www.ncbi.nlm.nih.gov/geo/query/acc.cgi?acc=GSE244052.
- Untargeted metabolomics data are publicly available through Metabolomics Workbench: PR002096; https://doi.org/10.21228/M8PJ8N.[60]
- This paper does not report original code.
- Any additional information required to reanalyze the data reported in this paper is available from the lead contact upon request.

AUTHOR CONTRIBUTIONS

A.S. and B.X. conceptualized the study. B.X. performed the experiments and analyzed the data. L.V.D. and O.K. contributed to the data processing and analysis. L.V.D. performed the qPCR experiments. B.X. wrote the original draft. A.Z. and V.L. performed the animal experiments and tissue collection. B.X., L.V.D., O.K., A.Z., V.L., and A.S. reviewed and edited the manuscript.

DECLARATION OF INTERESTS

The authors declare no competing interests.

STAR★METHODS

Detailed methods are provided in the online version of this paper and include the following:

- KEY RESOURCES TABLE
- EXPERIMENTAL MODEL AND STUDY PARTICIPANT DETAILS
  - Animal studies
- METHOD DETAILS
  - RNA-seq analysis
  - Untargeted metabolomics analysis
  - Omics data visualization and pathway analysis
  - Quantitative polymerase chain reaction (qPCR)
  - Immunohistochemistry
- QUANTIFICATION AND STATISTICAL ANALYSIS

SUPPLEMENTAL INFORMATION

Supplemental information can be found online at https://doi.org/10.1016/j.isci.2024.110901.

REFERENCES

1. Staruschenko, A. (2012). Regulation of transport in the connecting tubule and cortical collecting duct. Compr. Physiol. 2, 1541–1584. https://doi.org/10.1002/cphy.c110052.

2. Palygin, O., Pochynyuk, O., and Staruschenko, A. (2017). Role and mechanisms of regulation of the basolateral K(ir) 4.1/K(ir) 5.1K(+) channels in the distal tubules. Acta Physiol. 219, 260–273. https://doi.org/10.1111/apha.12703.

3. Palygin, O., Levchenko, V., Ilatovskaya, D.V., Pavlov, T.S., Pochynyuk, O.M., Jacob, H.J., Geurts, A.M., Hodges, M.R., and Staruschenko, A. (2017). Essential role of Kir5.1 channels in renal salt handling and blood pressure control. JCI Insight 2, e92331. https://doi.org/10.1172/jci.insight.92331.

4. Palygin, O., Pochynyuk, O., and Staruschenko, A. (2018). Distal tubule basolateral potassium channels: cellular and molecular mechanisms of regulation. Curr. Opin. Nephrol. Hypertens. 27, 373–378. https://doi.org/10.1097/mnh.0000000000000437.

5. Schlingmann, K.P., Renigunta, A., Hoorn, E.J., Forst, A.L., Renigunta, V., Atanasov, V., Mahendran, S., Barakat, T.S., Gillion, V., Godefroid, N., et al. (2021). Defects in KCNJ16 Cause a Novel Tubulopathy with Hypokalemia, Salt Wasting, Disturbed Acid-Base Homeostasis, and Sensorineural Deafness. J. Am. Soc. Nephrol. 32, 1498–1512. https://doi.org/10.1681/asn.2020111587.

6. Scholl, U.I., Choi, M., Liu, T., Ramaekers, V.T., Häusler, M.G., Grimmer, J., Tobe, S.W., Farhi, A., Nelson-Williams, C., and Lifton, R.P. (2009). Seizures, sensorineural deafness, ataxia, mental retardation, and electrolyte imbalance (SeSAME syndrome) caused by mutations in KCNJ10. Proc. Natl. Acad. Sci. USA 106, 5842–5847. https://doi.org/10.1073/pnas.0901749106.

7. Bockenhauer, D., Feather, S., Stanescu, H.C., Bandulik, S., Zdebik, A.A., Reichold, M., Tobin, J., Lieberer, E., Sterner, C., Landoure, G., et al. (2009). Epilepsy, ataxia, sensorineural deafness, tubulopathy, and KCNJ10 mutations. N. Engl. J. Med. 360, 1960–1970. https://doi.org/10.1056/NEJMoa0810276.

8. Webb, B.D., Hotchkiss, H., Prasun, P., Gelb, B.D., and Satlin, L. (2021). Biallelic loss-of-function variants in KCNJ16 presenting with hypokalemic metabolic acidosis. Eur. J. Hum. Genet. 29, 1566–1569. https://doi.org/10.1038/s41431-021-00883-0.

9. Dasinger, J.H., Walton, S.D., Burns, E.C., Cherian-Shaw, M., Abais-Battad, J.M., and Mattson, D.L. (2022). Impact of bedding on Dahl salt-sensitive hypertension and renal damage. Am. J. Physiol.-Renal. 323. F666–f672. https://doi.org/10.1152/ajprenal.00201.2022.

10. Lerman, L.O., Kurtz, T.W., Touyz, R.M., Ellison, D.H., Chade, A.R., Crowley, S.D., Mattson, D.L., Mullins, J.J., Osborn, J., Eirin, A., et al. (2019). Animal Models of Hypertension: A Scientific Statement From the American Heart Association. Hypertension 73, e87–e120. https://doi.org/10.1161/hyp.0000000000000090.

11. Kuczeriszka, M., and Wąsowicz, K. (2022). Animal models of hypertension: The status of nitric oxide and oxidative stress and the role of the renal medulla. Nitric Oxide 125–126, 40–46. https://doi.org/10.1016/j.niox.2022.06.003.

12. Kravtsova, O., Bohovyk, R., Levchenko, V., Palygin, O., Klemens, C.A., Rieg, T., and Staruschenko, A. (2022). SGLT2 inhibition effect on salt-induced hypertension, RAAS, and Na(+) transport in Dahl SS rats. Am. J. Physiol. Renal Physiol. 322. F692–f707. https://doi.org/10.1152/ajprenal.00053.2022.

13. Manis, A.D., Palygin, O., Khedr, S., Levchenko, V., Hodges, M.R., and Staruschenko, A. (2019). Relationship between the renin-angiotensin-aldosterone system and renal Kir5.1 channels. Clin. Sci. 133, 2449–2461. https://doi.org/10.1042/cs20190876.

14. Puissant, M.M., Muere, C., Levchenko, V., Manis, A.D., Martino, P., Forster, H.V., Palygin, O., Staruschenko, A., and Hodges, M.R. (2019). Genetic mutation of Kcnj16 identifies Kir5.1-containing channels as key regulators of acute and chronic pH homeostasis. FASEB J. 33, 5067–5075. https://doi.org/10.1096/fj.201802257R.

15. Manis, A.D., Cook-Snyder, D.R., Duffy, E., Osmani, W.A., Eilbes, M., Dillard, M., Palygin, O., Staruschenko, A., and Hodges, M.R. (2023). Repeated seizures lead to progressive ventilatory dysfunction in SS(Kcnj16-/-) rats. J. Appl. Physiol. 135, 872–885. https://doi.org/10.1152/japplphysiol.00072.2023.

16. Manis, A.D., Palygin, O., Isaeva, E., Levchenko, V., LaViolette, P.S., Pavlov, T.S., Hodges, M.R., and Staruschenko, A. (2021). Kcnj16 knockout produces audiogenic seizures in the Dahl salt-sensitive rat. JCI Insight 6, e143251. https://doi.org/10.1172/jci.insight.143251.

17. Arnett, D.K., and Claas, S.A. (2018). Omics of Blood Pressure and Hypertension. Circ. Res. 122, 1409–1419. https://doi.org/10.1161/circresaha.118.311342.

18. Arnett, D.K., and Graf, G.A. (2020). Metabolomics, Lipid Pathways, and Blood Pressure Change. Arterioscler. Thromb. Vasc. Biol. 40, 1801–1803. https://doi.org/10.1161/atvbaha.120.314816.

19. Jia, J., Yang, J.Q., Du, Y.R., Xu, Y., Kong, D., Zhang, X.L., Mao, J.H., Hu, G.F., Wang, K.H., and Kuang, Y.Q. (2022). Transcriptomic Profiling Reveals Underlying Immunoregulation Mechanisms of Resistant Hypertension in Injection Drug Users. J. Inflamm. Res. 15, 3409–3420. https://doi.org/10.2147/jir.S361634.

20. Louca, P., Nogal, A., Moskal, A., Goulding, N.J., Shipley, M.J., Alkis, T., Lindbohm, J.V.,

Hu, J., Kifer, D., Wang, N., et al. (2022). Cross-Sectional Blood Metabolite Markers of Hypertension: A Multicohort Analysis of 44,306 Individuals from the COnsortium of METabolomics Studies. Metabolites 12, 601. https://doi.org/10.3390/metabo12070601.

21. Zeller, T., Schurmann, C., Schramm, K., Müller, C., Kwon, S., Wild, P.S., Teumer, A., Herrington, D., Schillert, A., Iacoviello, L., et al. (2017). Transcriptome-Wide Analysis Identifies Novel Associations With Blood Pressure. Hypertension 70, 743–750. https://doi.org/10.1161/hypertensionaha.117.09458.

22. Rinschen, M.M., Palygin, O., Guijas, C., Palermo, A., Palacio-Escat, N., Domingo-Almenara, X., Montenegro-Burke, R., Saez-Rodriguez, J., Staruschenko, A., and Siuzdak, G. (2019). Metabolic rewiring of the hypertensive kidney. Sci. Signal. 12, eaax9760. https://doi.org/10.1126/scisignal.aax9760.

23. Gamba, G. (2023). Thirty years of the NaCl cotransporter: from cloning to physiology and structure. Am. J. Physiol.-Renal. 325, F479–F490. https://doi.org/10.1152/ajprenal.00114.2023.

24. Castañeda-Bueno, M., Ellison, D.H., and Gamba, G. (2022). Molecular mechanisms for the modulation of blood pressure and potassium homeostasis by the distal convoluted tubule. EMBO Mol. Med. 14, e14273. https://doi.org/10.15252/emmm.202114273.

25. Sagar, N.A., Tarafdar, S., Agarwal, S., Tarafdar, A., and Sharma, S. (2021). Polyamines: Functions, Metabolism, and Role in Human Disease Management. Med. Sci. 9, 44. https://doi.org/10.3390/medsci9020044.

26. Wu, P., Gao, Z.X., Zhang, D.D., Su, X.T., Wang, W.H., and Lin, D.H. (2019). Deletion of Kir5.1 Impairs Renal Ability to Excrete Potassium during Increased Dietary Potassium Intake. J. Am. Soc. Nephrol. 30, 1425–1438. https://doi.org/10.1681/asn.2019010025.

27. Mattson, D.L. (2019). Immune mechanisms of salt-sensitive hypertension and renal end-organ damage. Nat. Rev. Nephrol. 15, 290–300. https://doi.org/10.1038/s41581-019-0121-z.

28. Rucker, A.J., Rudemiller, N.P., and Crowley, S.D. (2018). Salt, Hypertension, and Immunity. Annu. Rev. Physiol. 80, 283–307. https://doi.org/10.1146/annurev-physiol-021317-121134.

29. Wade, B., Abais-Battad, J.M., and Mattson, D.L. (2016). Role of immune cells in salt-sensitive hypertension and renal injury. Curr. Opin. Nephrol. Hypertens. 25, 22–27. https://doi.org/10.1097/mnh.0000000000000183.

30. Elijovich, F., Kleyman, T.R., Laffer, C.L., and Kirabo, A. (2021). Immune Mechanisms of Dietary Salt-Induced Hypertension and Kidney Disease: Harry Goldblatt Award for Early Career Investigators 2020. Hypertension 78, 252–260. https://doi.org/10.1161/hypertensionaha.121.16495.

31. Barbaro, N.R., Foss, J.D., Kryshtal, D.O., Tsyba, N., Kumaresan, S., Xiao, L., Mernaugh, R.L., Itani, H.A., Loperena, R., Chen, W., et al. (2017). Dendritic Cell Amiloride-Sensitive Channels Mediate Sodium-Induced Inflammation and Hypertension. Cell Rep. 21, 1009–1020. https://doi.org/10.1016/j.celrep.2017.10.002.

32. Van Beusecum, J.P., Barbaro, N.R., McDowell, Z., Aden, L.A., Xiao, L., Pandey, A.K., Itani, H.A., Himmel, L.E., Harrison, D.G., and Kirabo, A. (2019). High Salt Activates CD11c(+) Antigen-Presenting Cells via SGK (Serum Glucocorticoid Kinase) 1 to Promote Renal Inflammation and Salt-Sensitive Hypertension. Hypertension 74, 555–563. https://doi.org/10.1161/hypertensionaha.119.12761.

33. Lu, X., and Crowley, S.D. (2022). The Immune System in Hypertension: a Lost Shaker of Salt 2021 Lewis K. Dahl Memorial Lecture. Hypertension 79, 1339–1347. https://doi.org/10.1161/hypertensionaha.122.18554.

34. Krishnan, S.M., Ling, Y.H., Huuskes, B.M., Ferens, D.M., Saini, N., Chan, C.T., Diep, H., Kett, M.M., Samuel, C.S., Kemp-Harper, B.K., et al. (2019). Pharmacological inhibition of the NLRP3 inflammasome reduces blood pressure, renal damage, and dysfunction in salt-sensitive hypertension. Cardiovasc. Res. 115, 776–787. https://doi.org/10.1093/cvr/cvy252.

35. Ertuglu, L.A., Mutchler, A.P., Yu, J., and Kirabo, A. (2022). Inflammation and oxidative stress in salt sensitive hypertension; The role of the NLRP3 inflammasome. Front. Physiol. 13, 1096296. https://doi.org/10.3389/fphys.2022.1096296.

36. Qi, J., Yu, X.J., Shi, X.L., Gao, H.L., Yi, Q.Y., Tan, H., Fan, X.Y., Zhang, Y., Song, X.A., Cui, W., et al. (2016). NF-κB Blockade in Hypothalamic Paraventricular Nucleus Inhibits High-Salt-Induced Hypertension Through NLRP3 and Caspase-1. Cardiovasc. Toxicol. 16, 345–354. https://doi.org/10.1007/s12012-015-9344-9.

37. Tian, Z., and Liang, M. (2021). Renal metabolism and hypertension. Nat. Commun. 12, 963. https://doi.org/10.1038/s41467-021-21301-5.

38. Zhang, F., Xie, Y., Yang, X., Peng, W., Qi, H., Li, B., Wen, F., Li, P., Sun, Y., and Zhang, L. (2023). Association of Serum Metabolites and Salt Sensitivity of Blood Pressure in Chinese Population: The EpiSS Study. Nutrients 15, 690. https://doi.org/10.3390/nu15030690.

39. Shi, M., He, J., Li, C., Lu, X., He, W.J., Cao, J., Chen, J., Chen, J.C., Bazzano, L.A., Li, J.X., et al. (2022). Metabolomics study of blood pressure salt-sensitivity and hypertension. Nutr. Metab. Cardiovasc. Dis. 32, 1681–1692. https://doi.org/10.1016/j.numecd.2022.04.002.

40. Rinschen, M.M., Palygin, O., El-Meanawy, A., Domingo-Almenara, X., Palermo, A., Dissanayake, L.V., Golosova, D., Schafroth, M.A., Guijas, C., Demir, F., et al. (2022). Accelerated lysine metabolism conveys kidney protection in salt-sensitive hypertension. Nat. Commun. 13, 4099. https://doi.org/10.1038/s41467-022-31670-0.

41. Shimada, S., Hoffmann, B.R., Yang, C., Kurth, T., Greene, A.S., Liang, M., Dash, R.K., and Cowley, A.W., Jr. (2023). Metabolic Responses of Normal Rat Kidneys to a High Salt Intake. Function (Oxf) 4, zqad031. https://doi.org/10.1093/function/zqad031.

42. Lewis, S., Chen, L., Raghuram, V., Khundmiri, S.J., Chou, C.L., Yang, C.R., and Knepper, M.A. (2021). "SLC-omics" of the kidney: solute transporters along the nephron. Am. J. Physiol. Cell Physiol. 321, C507–c518. https://doi.org/10.1152/ajpcell.00197.2021.

43. Huang, R.Z., Ma, J.F., Chen, S., Chen, Y.M., Fang, A.P., Lu, X.T., Huang, Z.H., Zhu, H.L., and Huang, B.X. (2023). Associations of serum betaine with blood pressure and hypertension incidence in middle-aged and older adults: a prospective cohort study. Food Funct. 14, 4881–4890. https://doi.org/10.1039/d3fo00325f.

44. Vasdev, S., Singal, P., and Gill, V. (2009). The antihypertensive effect of cysteine. Int. J. Angiol. 18, 7–21. https://doi.org/10.1055/s-0031-1278316.

45. Raasch, W., Schäfer, U., Qadri, F., and Dominiak, P. (2002). Agmatine, an endogenous ligand at imidazoline binding sites, does not antagonize the clonidine-mediated blood pressure reaction. Br. J. Pharmacol. 135, 663–672. https://doi.org/10.1038/sj.bjp.0704513.

46. Tian, Z., Liu, Y., Usa, K., Mladinov, D., Fang, Y., Ding, X., Greene, A.S., Cowley, A.W., Jr., and Liang, M. (2009). Novel role of fumarate metabolism in dahl-salt sensitive hypertension. Hypertension 54, 255–260. https://doi.org/10.1161/hypertensionaha.109.129528.

47. Xue, H., Geurts, A.M., Usa, K., Wang, F., Lin, Y., Phillips, J., Henderson, L., Baker, M.A., Tian, Z., and Liang, M. (2019). Fumarase Overexpression Abolishes Hypertension Attributable to endothelial NO synthase Haploinsufficiency in Dahl Salt-Sensitive Rats. Hypertension 74, 313–322. https://doi.org/10.1161/hypertensionaha.119.12723.

48. Hou, E., Sun, N., Zhang, F., Zhao, C., Usa, K., Liang, M., and Tian, Z. (2017). Malate and Aspartate Increase L-Arginine and Nitric Oxide and Attenuate Hypertension. Cell Rep. 19, 1631–1639. https://doi.org/10.1016/j.celrep.2017.04.071.

49. Sadagopan, N., Li, W., Roberds, S.L., Major, T., Preston, G.M., Yu, Y., and Tones, M.A. (2007). Circulating succinate is elevated in rodent models of hypertension and metabolic disease. Am. J. Hypertens. 20, 1209–1215. https://doi.org/10.1016/j.amjhyper.2007.05.010.

50. Abukhodair, A.W., Abukhudair, W., and Alqarni, M.S. (2021). The Effects of L-Arginine in Hypertensive Patients: A Literature Review. Cureus 13, e20485. https://doi.org/10.7759/cureus.20485.

51. Vasdev, S., and Gill, V. (2008). The antihypertensive effect of arginine. Int. J. Angiol. 17, 7–22. https://doi.org/10.1055/s-0031-1278274.

52. Singh, P., Gollapalli, K., Mangiola, S., Schranner, D., Yusuf, M.A., Chamoli, M., Shi, S.L., Lopes Bastos, B., Nair, T., Riermeier, A., et al. (2023). Taurine deficiency as a driver of aging. Science 380, eabn9257. https://doi.org/10.1126/science.abn9257.

53. Sun, Q., Wang, B., Li, Y., Sun, F., Li, P., Xia, W., Zhou, X., Li, Q., Wang, X., Chen, J., et al. (2016). Taurine Supplementation Lowers Blood Pressure and Improves Vascular Function in Prehypertension: Randomized, Double-Blind, Placebo-Controlled Study. Hypertension 67, 541–549. https://doi.org/10.1161/hypertensionaha.115.06624.

54. Dornas, W.C., Cardoso, L.M., Silva, M., Machado, N.L.S., Chianca, D.A., Jr., Alzamora, A.C., Lima, W.G., Lagente, V., and Silva, M.E. (2017). Oxidative stress causes hypertension and activation of nuclear factor-κB after high-fructose and salt treatments. Sci. Rep. 7, 46051. https://doi.org/10.1038/srep46051.

55. Pavlov, T.S., Palygin, O., Isaeva, E., Levchenko, V., Khedr, S., Blass, G., Ilatovskaya, D.V., Cowley, A.W., Jr., and Staruschenko, A. (2020). NOX4-dependent regulation of ENaC in hypertension and diabetic kidney disease. FASEB J. 34, 13396–13408. https://doi.org/10.1096/fj.202000966RR.

56. Wilcox, C.S. (2003). Redox regulation of the afferent arteriole and tubuloglomerular feedback. Acta Physiol. Scand. *179*, 217–223. https://doi.org/10.1046/j.0001-6772.2003.01205.x.

57. Araujo, M., and Wilcox, C.S. (2014). Oxidative stress in hypertension: role of the kidney. Antioxid. Redox Signal. *20*, 74–101. https://doi.org/10.1089/ars.2013.5259.

58. Ramachandran, J., and Peluffo, R.D. (2017). Threshold levels of extracellular l-arginine that trigger NOS-mediated ROS/RNS production in cardiac ventricular myocytes. Am. J. Physiol. Cell Physiol. *312*. C144–c154. https://doi.org/10.1152/ajpcell.00150.2016.

59. Pietrowski, E., Bender, B., Huppert, J., White, R., Luhmann, H.J., and Kuhlmann, C.R.W. (2011). Pro-inflammatory effects of interleukin-17A on vascular smooth muscle cells involve NAD(P)H- oxidase derived reactive oxygen species. J. Vasc. Res. *48*, 52–58. https://doi.org/10.1159/000317400.

60. Sud, M., Fahy, E., Cotter, D., Azam, K., Vadivelu, I., Burant, C., Edison, A., Fiehn, O., Higashi, R., Nair, K.S., et al. (2016). Metabolomics Workbench: An international repository for metabolomics data and metadata, metabolite standards, protocols, tutorials and training, and analysis tools. Nucleic Acids Res. *44*, D463–D470. https://doi.org/10.1093/nar/gkv1042.

61. Hale, V.L., Jeraldo, P., Mundy, M., Yao, J., Keeney, G., Scott, N., Cheek, E.H., Davidson, J., Greene, M., Martinez, C., et al. (2018). Synthesis of multi-omic data and community metabolic models reveals insights into the role of hydrogen sulfide in colon cancer. Methods *149*, 59–68. https://doi.org/10.1016/j.ymeth.2018.04.024.

62. Xyda, S.E., Vuckovic, I., Petterson, X.M., Dasari, S., Lalia, A.Z., Parvizi, M., Macura, S.I., and Lanza, I.R. (2020). Distinct Influence of Omega-3 Fatty Acids on the Plasma Metabolome of Healthy Older Adults. J. Gerontol. A Biol. Sci. Med. Sci. *75*, 875–884. https://doi.org/10.1093/gerona/glz141.

63. Pang, Z., Chong, J., Zhou, G., de Lima Morais, D.A., Chang, L., Barrette, M., Gauthier, C., Jacques, P.É., Li, S., and Xia, J. (2021). MetaboAnalyst 5.0: narrowing the gap between raw spectra and functional insights. Nucleic Acids Res. *49*. W388–w396. https://doi.org/10.1093/nar/gkab382.

64. Zietara, A., Palygin, O., Levchenko, V., Dissanayake, L.V., Klemens, C.A., Geurts, A., Denton, J.S., and Staruschenko, A. (2023). K(ir)7.1 knockdown and inhibition alter renal electrolyte handling but not the development of hypertension in Dahl salt-sensitive rats. Am. J. Physiol. Renal Physiol. *325*, F177–F187. https://doi.org/10.1152/ajprenal.00059.2023.

65. Ishiguro, T., Takeda, J., Fang, X., Bronson, H., and Olson, D.M. (2016). Interleukin (IL)-1 in rat parturition: IL-1 receptors 1 and 2 and accessory proteins abundance in pregnant rat uterus at term - regulation by progesterone. Physiol. Rep. *4*, e12866. https://doi.org/10.14814/phy2.12866.

STAR★METHODS

KEY RESOURCES TABLE

REAGENT or RESOURCE	SOURCE	IDENTIFIER
Antibodies		
Kallikrein 1	ABcloncal	Cat#: A1807; RRID: AB_2763846
Carbonic anhydrase 3	ABcloncal	Cat#: A1212; RRID: AB_2759010
Osteopontin	Proteintech	Cat#: 22952-1-AP; RRID: AB_2783651
Chemicals, peptides, and recombinant proteins		
TRIzol	ThermoFisher	Cat# 15596026
BSA	Sigma	Cat# A3059
Deposited data		
Raw data (Transcriptomics)	This paper	GEO: GSE244052
Raw data (Untargeted metabolomics)	This paper	Metabolomics Workbench: PR002096
Experimental models: organisms/strains		
Rat: SS-Kcnj16em1Mcwi	MCW	Rat Genome Database ID: 6893434
Oligonucleotides		
See Table S5	N/A	N/A
Software and algorithms		
Graphpad Prism v10	GraphPad software	N/A
Ingenuity Pathway Analysis	Qiagen	N/A
Other		
0.4% NaCl diet	Dyets	No. D113756

EXPERIMENTAL MODEL AND STUDY PARTICIPANT DETAILS

Animal studies

Animal use and welfare procedures adhered to the National Institute of Health Guide for the Care and Use of Laboratory Animals following protocols reviewed and approved by the University of South Florida Institutional Animal Care and Use Committee. All experiments were carried out in accordance with relevant guidelines and regulations and in compliance with the ARRIVE guidelines. Male *Kcnj16* knock-out (KO) rats and wild-type Dahl SS (WT) rats were initially acquired from colonies sustained at the Medical College of Wisconsin and bred and maintained at the University of South Florida.[3,13] Rats were housed in controlled environmental conditions under a 12-hour-light/dark cycle with food (0.4% NaCl diet, Dyets Inc., D113755) and water provided *ad libitum*. At the age of 11–12 weeks old, rats were placed in metabolic cages for 24-h urine collection. Prior to euthanasia, rats were anesthetized with isoflurane for arterial blood collection as well as kidney flushing with PBS. The left kidneys were removed and used for subsequent RNA-Seq and untargeted metabolomic analysis.

METHOD DETAILS

RNA-seq analysis

Total RNA from flash-frozen cortical kidney sections of WT (N = 5) and KO rats (N = 5) was isolated using TRIzol Reagent (Invitrogen, USA) following the manufacture's protocol and sent to Novogene Co, China, for quality control and RNA-Sequencing.

RNA integrity was assessed using RNA Nano 6000 Assay Kit of the Bioanalyzer 2100 system (Agilent Technologies, CA, USA). For library preparation, mRNA was first purified from total RNA using poly-T oligo-attached magnetic beads. After fragmentation, the first strand cDNA was synthesized using random hexamer primers, followed by the second strand cDNA synthesized using either dUTP for the directional library or dTTP for the non-directional library. The library was checked with Qubit and real-time PCR for quantification and Agilent Bioanalyzer 2100 system for size distribution detection. Then, the clustering of the index-coded samples was performed on a cBot Cluster Generation System using TruSeq PE Cluster Kit v3-cBot-HS (Ilumina, USA)) according to the manufacturer's instructions. After cluster generation, the library preparations were sequenced on an Illumina Novaseq platform and 150 bp paired-end reads were generated. Sequencing reads were aligned to the rat Rnor_6.0.98 (Ensemble) transcriptome and differential expression analysis of genes was performed using the DESeq2 R package (1.20.0). Genes with an adjusted p-value of 0.05 were set as the threshold for significantly differential expression.

Untargeted metabolomics analysis

Flash frozen kidney tissue, urine and plasma from arterial blood of WT (N = 5) and KO (N = 6) rats were sent to Mayo Clinical Metabolomics Core (Rochester, MN, USA) for untargeted metabolomics analysis.[61,62] Briefly, processed samples were divided into 2 aliquots and dried down for analysis on a Quadrupole Time-of-Flight Mass Spectrometer (Agilent Technologies 6550 Q-TOF) coupled with an Ultra High Pressure Liquid Chromatograph (Agilent Technologies 1290 Infinity UHPLC). Profiling data were acquired under both positive and negative electrospray ionization conditions over a mass range of 100–1200 m/z at a resolution of 10,000–35,000 (separate runs). Metabolite separation was achieved using two columns of differing polarity, a hydrophilic interaction column (HILIC, ethylene-bridged hybrid 2.1 × 150 mm, 1.7 μm; waters) and a reversed-phase C18 column (high-strength silica 2.1 × 150 mm, 1.8 μm; Waters). For each column, the run time is 20 min using a flow rate of 400 μL/min. A total of four samples per run was performed to give maximum coverage of metabolites. Samples were injected in duplicate or triplicate, and a quality control sample, made up of a subset of samples from the study was injected several times during a run. All raw data files obtained were converted to compound exchange file format using Masshunter DA reprocessor software (Agilent, USA). Mass Profile Professional (Agilent, USA) was used for data alignment and to convert each metabolite feature (m/z x intensity x time) into a matrix of detected peaks for compound identification. Components that were matched were further examined by comparison to a purchased reference standard of the proposed compound. Mass accuracy of the Q-TOF method was <5ppm with retention time precision better than 0.2%. A 1.2x fold change can be detected with a precision of 4%.

To filter low intensity hits, a metabolite must have peak intensity of at least 5000 in at least 75% samples to be eligible for downstream analyses. Data normalization and differential expression analysis were performed by MetaboanalystR (FDR adjusted p-value ≤ 0.05). Metabolites detected by different modes were combined together. When compounds were detected by different modes, the mode that detects the highest peak intensity of the compound was chosen.

Omics data visualization and pathway analysis

Heatmaps (transcriptomic and metabolomic data) and volcano plot (transcriptomic data) were generated using R packages by Novogene. Orthogonal Projections to Latent Structures Discriminant Analysis (OPLS-DA) of metabolomic data were performed by MetaboAnalyst5.0.[63] Further pathway and functional analysis were done using Ingenuity Pathway Analysis (QIAGEN Inc., Germany).

Quantitative polymerase chain reaction (qPCR)

qPCR was performed as previous described.[64] Briefly, total RNA was extracted from kidney cortex using TRIzol reagent (Thermo Fisher Scientific) and quantified using a Synergy *Neo*2 plate reader (BioTek). 1 μg RNA of each sample was used to produce cDNA using a Revert Aid First Strand cDNA Synthesis Kit (Thermo Fisher Scientific). qPCR was performed using QuantStudio 6 Pro (Applied Biosystemes, Thermo Fisher Scientific) with Maxima SYBR Green/ROX qPCR Master Mix (Thermo Fisher Scientific). The relative mRNA quantification was determined by normalizing it to 18s. All end products were sequenced to ensure accuracy. The primers used are listed in Table S5. All primers in this paper were designed using NCBI primer blast tool except for *Il1b*[65] which was previously published.

Immunohistochemistry

Immunohistochemistry analysis was performed as previously described.[3] Briefly, formalin-fixed, paraffin-embedded right kidneys were cut at 4 μm, dried, and deparatffinized. The slides were then treated with a citrate buffer (pH 6) followed by incubation with peroxidase block, avidin block, biotin block and serum-free protein block. The slides were incubated with primary antibodies (see key resources table) for 90 min. The dilutions of antibodies are: Kallikrein 1 (1:500), Carbonic anhydrase 3 (1:200), Osteopontin (1:500). After incubating with secondary antibodies, all slides were counterstained with Mayer's hematoxylin, dehydrated, and mounted with permanent mounting medium.

The protein abuance were quantified by color thresholding using Qupath (Qupath v.0.4.2). For each rat, at least 19 cortical areas of the kidney were randomly selected. The protein abundance were then quantified as the percentage of area with positive staining.

QUANTIFICATION AND STATISTICAL ANALYSIS

Data are expressed as mean ± SEM and plotted by GraphPad Prism 10 (GraphPad Software, San Diego, CA). Different groups were compared using the Student's t test by Microsoft Excel or GraphPad Prism 10. *p < 0.05, **p < 0.01, ***p < 0.001, ****p < 0.0001.